Heliyon 9 (2023) e20512

Contents lists available at ScienceDirect

Heliyon

journal homepage: www.cell.com/heliyon

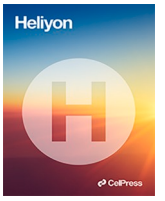

Enhanced NLO response and switching self-focussing in benzodiazepine derivative with $–NO_2$ and -Br substitution

Aswathy P [a], I. Hubert Joe [b,*], B. Narayana [c], B.K. Sarojini [d], K.R. Harshitha [d], J. Clemy Monicka [e]

[a] Department of Physics, University of Kerala, Kariavattom, Thiruvananthapuram- 695581, India
[b] Department of Nanoscience and Nanotechnology, University of Kerala, Kariavattom, Thiruvananthapuram- 695581, India
[c] Department of Chemistry, Mangalore University, Mangalagangothri 574199, India
[d] Department of Studies in Industrial Chemistry, Mangalore University, Mangalagangothri, 574199, India
[e] Department of Physics, St. John's College of Arts and Science, M.S.University, Kanyakumari-629204, Tamil Nadu, India

ARTICLE INFO

Keywords:
DFT
NCA
NBO
MEP
Tauc's plot
Z-scan

ABSTRACT

Optoelectronic and the cubic nonlinear optical properties of 4-(4-Bromophenyl)-2-(4-nitrophenyl)-2, 3-dihydro-1H-1, 5-benzodiazepine have been studied. Z-scan technique was used for the third-order nonlinear optical measurements namely, nonlinear absorption, nonlinear refraction, and optical power limiting behaviour employing an Nd: YAG laser of 532 nm wavelength having 5 ns Gaussian pulses. B3LYP/6–311 ++ G (d, p) level of theory was employed for structural optimization, vibrational wavenumber, frontier molecular orbitals, natural bond orbital and population analysis. The MOLVIB programme was used to perform unambiguous vibrational assignments based on potential energy distribution values acquired from normal coordinate analysis. B3LYP and CAM-B3LYP hybrid functions have been employed at the DFT level to calculate the theoretical second-order hyperpolarizability. The substitution of $–NO_2$ and -Br in this benzodiazepine compound enhances the second-order hyperpolarizability (γ) to the order of 10^{-34} esu and, switching of self-defocussing to self-focussing phenomenon. The HOMO-LUMO and optical band gap analysis illustrates that polarizing nature of the molecule vary with substituents. The obtained results indicate that this compound has potential applications in optoelectronics and photonics.

1. Introduction

Recently, the scientific community has concentrated on enhancing materials' third-order nonlinear optical (NLO) properties for creating NLO gadgets in optoelectronic and photonics applications [1,2]. Organic NLO materials have recently been the focus of experimental and computational researchers due to their potential uses in modern technologies [3]. The enormous structural variety, broadband optical response, and higher NLO parameters are some of the few advantages of organic materials over inorganic or hybrid materials. Inorganic oxide compounds are much more stable at high temperatures, certain complex iron oxides with excellent electronic properties are found to be promising materials for NLO applications [4,5]. Modifying molecular hyperpolarizabilities is the key concern in the development of new NLO materials [6–8]. Functional group modification, metal doping, donor-acceptor combinations,

* Corresponding author.
E-mail address: hubertjoe@keralauniversity.ac.in (I.H. Joe).

https://doi.org/10.1016/j.heliyon.2023.e20512
Received 25 July 2023; Received in revised form 19 September 2023; Accepted 27 September 2023
Available online 30 September 2023

bond length variations, and other structural modification techniques control the NLO response [9–18]. Diazepine derivatives are organic compounds having five carbon atoms along with two nitrogen atoms in the same ring [19–21]. Furthermore, the existence of a N–H group and substituent phenyl rings results in the formation of π-conjugated electron system, i.e., a donor-π-acceptor group, which triggers the NLO response in these derivatives [22–26]. Also, the substitution of functional groups like halogens, nitro entities and designing thin film may enhance the NLO activity of the benzodiazepine derivatives. However, reports on computational along with experimental NLO studies of benzodiazepine-based compounds are rare. Hence, there is a growing interest in figuring out the structural and spectroscopic features of these compounds. A detailed overview of the compound's behavior at the molecular level is obtained by combining theoretical and experimental methodologies.

Third-order NLO properties of 4-(4-Bromophenyl)-2- (4-nitrophenyl) −2, 3-dihydro-1H-1, 5 benzodiazepine (12D) using both experimental and computational methodologies are reported in this work is first-hand according to the literature reviewed. This molecule's novelty for nonlinear optical (NLO) study results from its distinct structural characteristics which contribute to enhanced NLO effects. It possesses a combination of electron-donating (nitro) and electron-withdrawing (bromine) entities on its aromatic rings. This type of push-pull system can lead to an asymmetrical electron distribution within the molecule, creating a significant dipole moment and potentially enhancing its nonlinear optical properties. The push-pull effect can cause transfer of charges across the electron-rich and electron-deficient units, resulting in a substantial molecular hyperpolarizability. The theoretical investigations were

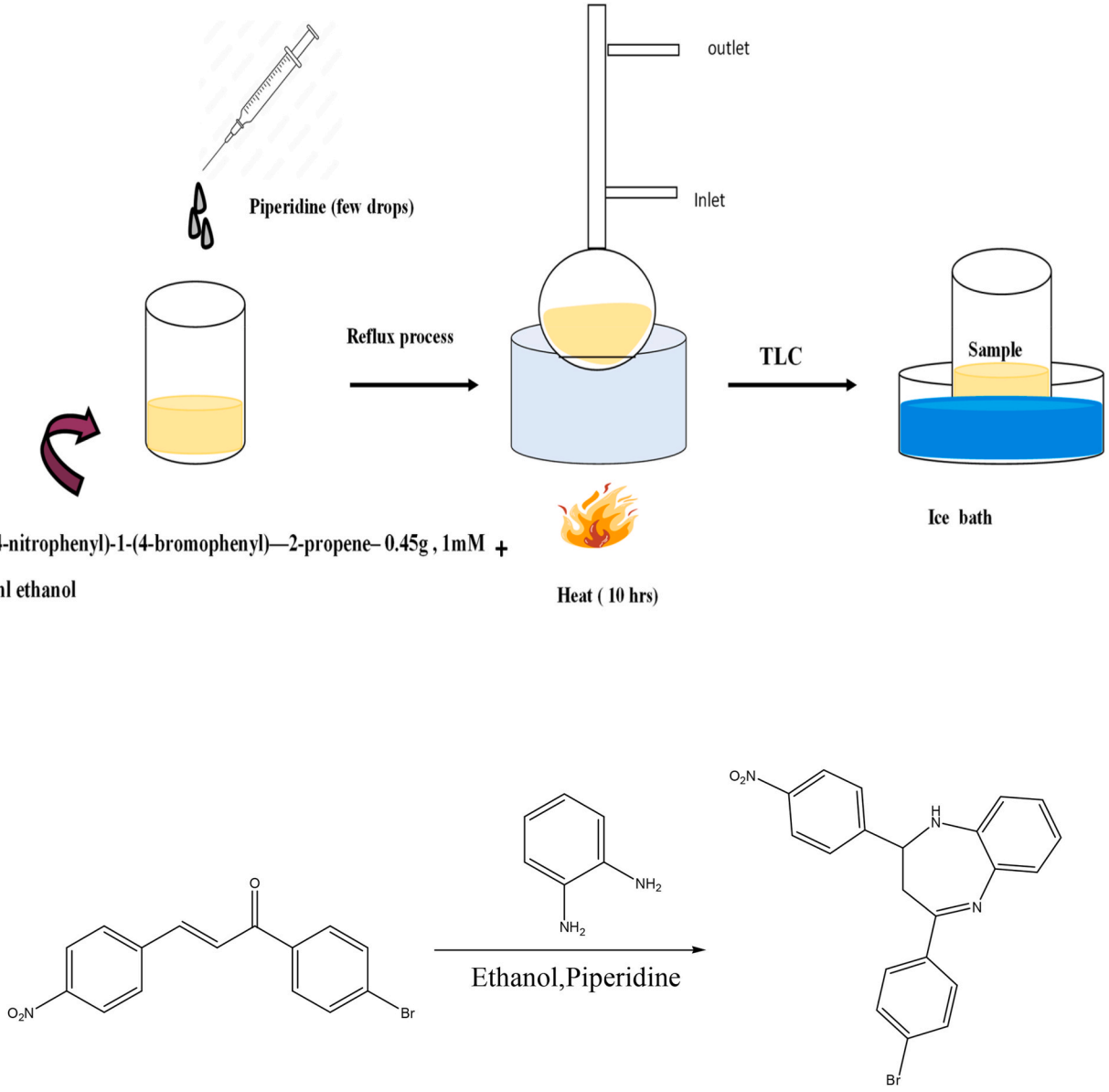

Fig. 1. Schematic diagram of material synthesis.

performed using DFT analyses. Z-scan method was used for determining the NLO characteristics; nonlinear refractive index (NLR), non-linear absorption coefficient (NLA), second–order hyperpolarizability, and optical limiting.

2. Material synthesis

A mixture of 3-(4-nitrophenyl)-1-(4-bromophenyl)-2-propene (0.45g, 0.001 M) in 30 ml ethanol and a scarce amount of piperidine was refluxed with 1,2-diaminobenzene (0.258g, 0.001 M) for 10hrs. The end of the process was identified by TLC method, further cooled, and quenched with ice water. The residue was filtered and dried to get the final product. The schematic diagram is shown in Fig. 1.

3. Instrumentation

The NMR analysis was performed using Bruker Advance 400 MHz NMR spectrometer with methanol as solvent. Raman spectrum was generated with Horiba LabRam HR evolution Raman spectrophotometer and FT-IR spectra using a PerkinElmer Spectrophotometer. The UV–visible absorption spectrum was generated using Jasco V-750 spectrophotometer. Fluoromax4 Horiba Scientific spectrophotometer was used to study the emission spectrum.The z-scan instrumentation is cited elsewhere [27].

4. Computational details

Quantum chemical calculations were done for the 12D molecule with functional (B3LYP), and the 6–311 ++ G (d, p) basis set using the Gaussian 09 software [28,29]. MOLVIB 7.0 programme was used to assess the potential energy distribution (PED) using the scaled quantum mechanical force field (SQMFF) method [30,31], it is utilized to assign certain vibrational assignments when comparing theoretical vibrational spectra for 12D to actual FT-IR and FT-Raman spectra. Electronic absorption spectra in polar and nonpolar solvent phases were modelled using the TD-DFT/6–311 ++ G (d, p) approach. The intermolecular bonding and interactions were understood using Natural Bond Orbital (NBO) studies. The computational prediction of dipole moment and hyperpolarizabilities at the 532 nm wavelength were obtained using hybrid functional B3LYP and CAM (Coulomb Attenuated Method)-B3LYP with the same basis

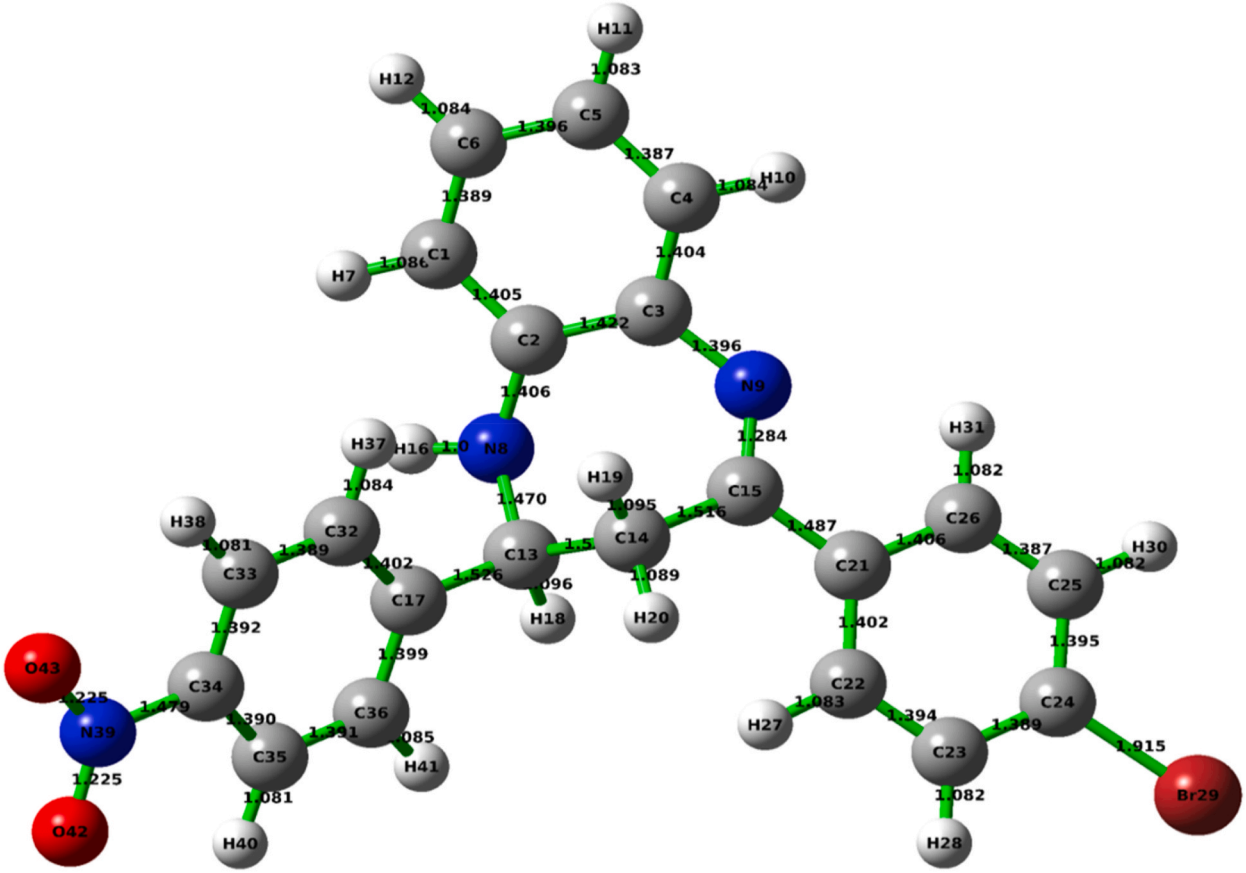

Fig. 2. Optimized structure of 12D.

set.

5. Observations and interpretation

5.1. NMR analysis

^{1}H HNMR and ^{13}C NMR were done to understand the elemental constituents with methanol as the solvent and the interpretation data is given below.^{1}H NMR (Methanol, 400 MHz): δ 3.00–3.05 (dd, 1H, CH_2-H_A, $J_{AX} = 3.68$Hz, $J_{AB} = 13.73$ Hz), δ 3.07–3.13 (dd, 1H, CH_2-H_B, $J_{BX} = 6.92$ Hz, $J_{BA} = 13.73$Hz), δ 5.22–5.24 (t, 1H, CH-H_x, $J_{XA} = 3.2$Hz, $J_{XB} = 6.32$Hz), δ 5.88 (s, 1H, NH), δ 6.83–7.80 (m, 12H, Ar–H). 13C NMR (Methanol); 37.86 (CH_2), 67.88 (CH), 115.19 (d), 115.40 (d), 119.80, 120.65, 126.78, 128.49 (d), 129.45 (t), 136.03 (d), 137.76, 140.48, 141.87 (d),160.53, 162.46, 162.95, 164.92 (d). The chemical shift observed at δ(3.00–3.13) ppm and δ (5.22–5.24) ppm corresponds to the proton of CH_2 and CH group in the diazepine ring, respectively. The singlet at δ5.88 ppm corresponds to proton attached to the nitrogen atom. The chemical shift range δ6.83–7.80 ppm indicates that there are a total of 12 aromatic protons, which are likely part of a substituted benzene ring. From these ^{1}H and ^{13}C NMR confirms that 16 protons and 21 carbon atoms are present in the synthesized molecule.

5.2. Structural optimization

The structural optimization of 12D was computed using Gaussian 09W package, and the relaxed structure was visualized using 'Gauss view 5.0.8'. The compound's structure after optimization is depicted in Fig. 2.The minimum global energy was found to be −3698.91 Hartrees; the dipole moment was measured as 2.4 Debye, which confirms the charge distribution throughout the molecule. The geometrical parameters have been comparable to experimental parameters of a similar molecule [32]. In this optimized structure, the diazepine ring is having a distorted boat shape with an adequate mirror axis along C14 and the midpoint of the C3–C2 bond. The atoms N8 and N9 are not planar with the aryl rings with the torsion angle of N8–C2–C3–N9 is 0.207°. Because of the steric effect of the nitro-substitution, the atoms C21–C22 and C17–C32 are rotated off the plane of the diazepine ring. The elongation of C4–H10 (1.084 Å) results from the formation of C4–H10···N9 hydrogen bonding, and the lengthening of the bond of N8–H16 (1.011 Å) confirms the C14–H19···N8 hydrogen bonding. The slight variation in geometrical parameters results as the molecular optimization is done in a single molecule in gaseous phase; whereas the experimentally obtained are in a crystal environment, i.e. solid phase.

5.3. Theoretical hyperpolarizability calculations

Nonlinear optics (NLO) effects originate when an intense electromagnetic fields interact with dielectric media, resulting in new fields with differing phases, frequencies, amplitudes, or other transmission properties to the incoming field. Donor-acceptor substitution of π-conjugated molecules can change the properties of NLO materials. The NLO attributes of a single molecule such as polarizability, dipole moment (μ), and hyperpolarizability (γ) are theoretically obtained with the aid of DFT at B3LYP and CAM -B3LYP functional with the same basis set using finite field procedure [33]. The second-order hyperpolarizability $\gamma(-2\omega;\omega,\omega,0)$ at 532 nm is measured to be 126.27×10^{-34} esu and its values in different solvents and that of a similar compound are shown in Table 1.

5.4. Z-scan

The third-order NLO properties of 12D were analyzed by a Gaussian beam in open and closed aperture configurations of the z-scan technique [35,36]. The NLA coefficient and NLR are significant factors to consider while studying the NLO response of the medium. It was estimated at 3 mM concentration with an intensity of 7.01 GW/cm^2 in polar and nonpolar solvents.

5.4.1. 1 open (OA) and closed aperture (CA)

In OA method, the energy detector monitors the whole beam that goes through the sample, and it can be used to find the sign and magnitude of the compound's NLA coefficients in polar and nonpolar solvents. The OA curves of 12D in four solvents are plotted as normalized transmittance versus sample position through the beam focus from one side to the other (Fig. 3). The transmittance of all OA curves is symmetrical with reference to the focus (z = 0) and has the lowest value thereof; then increases and ultimately saturates,

Table 1
Theoretical hyperpolarizability values of 12D at B3LYP and CAM-B3LYP level.

Solvents	α (x10^{-24} esu)		β (x10^{-30} esu)		γ (x10^{-34} esu)		
	B3LYP	CAM-B3LYP	B3LYP	CAM-B3LYP	B3LYP	CAM-B3LYP	
Gas	48.95	46.63	740.83	833.988	3628.05	126.27	Present work
DMSO	57.6	52.87	905.83	990.74	3192.25	1882.53	
Methanol	56.7	52.22	884.02	973.45	3078.48	1763.17	
Toluene	56.19	52.14	890.05	958.26	3053.75	1649.76	
CCl_4	56.33	52.4	879.85	942.47	3011.68	1589.06	
BFBD-Gas	37.23	26.18	227.09	153.50	270.08	5.58	[34]

demonstrating an intensity-based absorption effect. A positive absorption coefficient is deduced because the transmittance valley in the OA curve indicates a significant reverse saturable absorption (RSA). This response could be due to a variety of absorption phenomena such as one-photon absorption along with excited state absorption (1 PA + ESA), two-photon absorption (2 PA), 2 PA along with ESA [37,38]. A band gap of 2.96 eV was obtained from Tauc's plot, the photon energy of the source is 2.66eV(532 nm). Since the condition for 2 PA is $E_g < 2h\nu < 2E_g$ ($2.96 < 4.66 < 5.92$) is satisfied, the prominent mechanism of absorption is 2 PA. However, due to the difference between the band gap (2.96 eV) and photon energy (2.33 eV), there is a possibility for the electrons in the first excited state (E_1) transferring to second virtual excited level E_2 (4.66eV), and to further excite to nearest available state (E_3) ($E_2 \rightarrow E_3$ non-radiative transition) as shown in Fig. 4, substantiating the mechanism to be 2 PA + ESA [39,40].

The CA method was utilized to assess the (NLR) index, n_2. The laser beam from the sample is allowed to pass through an aperture positioned in front of the detector to study the material's NLR index. Upon division of CA Z-scan data by OA data, the pure NLR index is found out [41].The valley-peak configuration represents a positive NLR index, signifying a self-focussing phenomenon and a positive refractive index as shown in Fig. 5. The calculated values of β, n_2, Re $\chi^{(3)}$, Im $\chi^{(3)}$, $\chi^{(3)}$ and γ are tabulated and also the previously reported values are shown in Table 2

The experimental second-order hyperpolarizability is high in DMSO solvent than the nonpolar solvents; indicates that strong polar solvents will exhibit better polarizability, also the pure solvents alone doesn't show any nonlinearity in z-scan measurements. Comparing similar benzodiazepine derivatives, the obtained value of γ is an order higher than the BFBD diazepine derivative which is observed under the same experimental states (concentration, intensity, and excitation wavelength) [34]. In CA curves, the sign of the NLR index switches from negative to positive via substitution of strong electron-withdrawing moiety(-NO_2) at the ortho position of the phenyl ring attached to the benzodiazepine ring. The replacement of fluorine atoms by Br and NO_2 in the compound results in a higher γ value than the reported compounds of similar structure [42]. The electron-accepting ability of NO_2 group enhances the polarization and leads to the switching of self-defocussing effect to self-focussing. The halogen substitution varies the NLO parameters in increasing order of F < Cl < Br < I [43–46]. The third-order NLO properties of a molecule are governed by its cubic nonlinear susceptibility, which is the extend of the molecule's capability to respond to an external electric field. Since both electron-donating and withdrawing entities are present in the molecule's aromatic improves its third-order NLO response. The second–order hyperpolarizability measurements give a value of $(2.40–0.3) \times 10^{-34}$ esu. The computed second-order hyperpolarizability using CAM-B3LYP functional with 6–311++G (d, p) basis set in DMSO solvent shows improved result than the B3LYP functional. The computational results lies close by the experimental one, a small deviation in the experimental results depends on concentration of the solution, intensity of the beam pulse

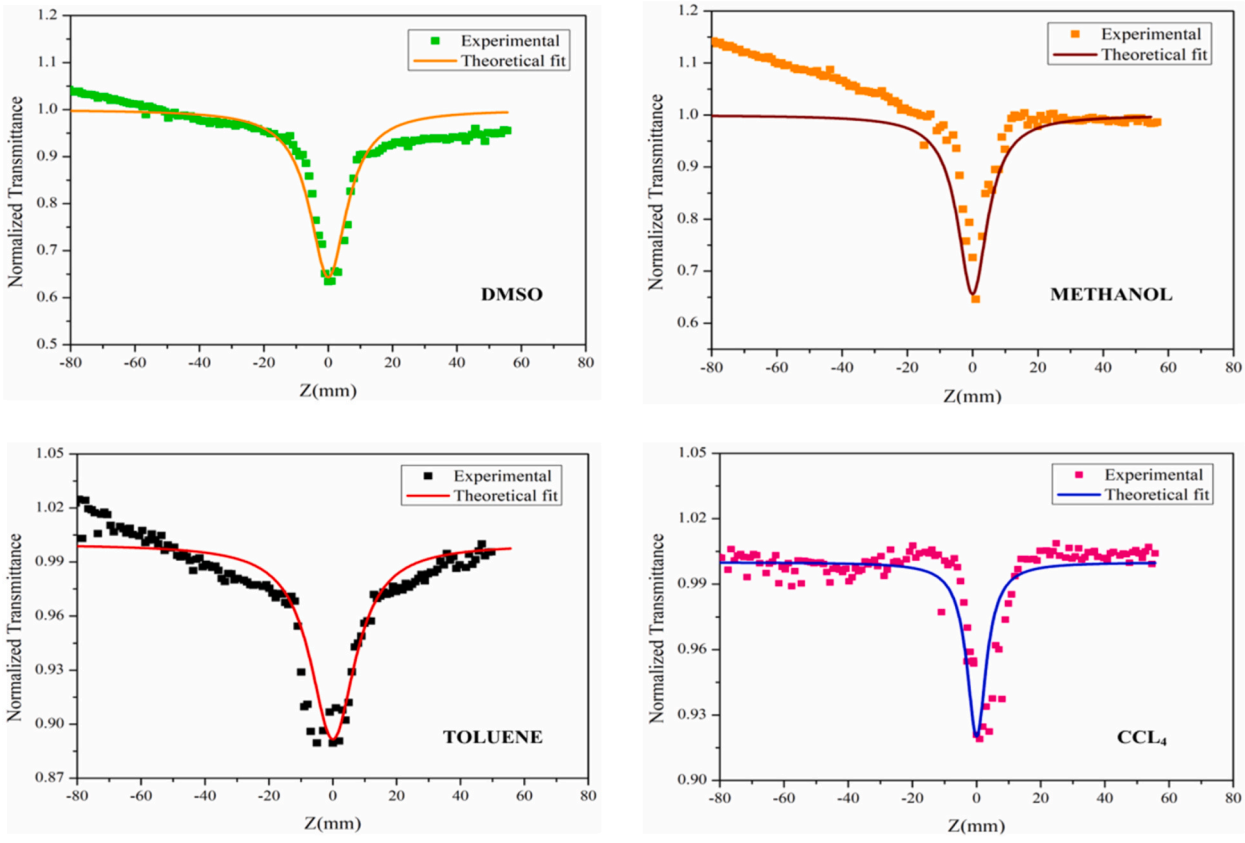

Fig. 3. OA Z-scan curves of 12D.

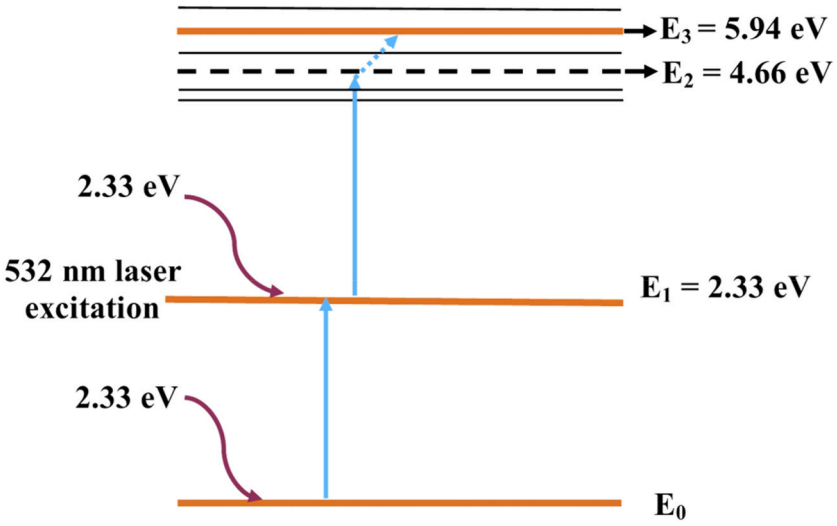

Fig. 4. 2 PA and ESA energy level representation.

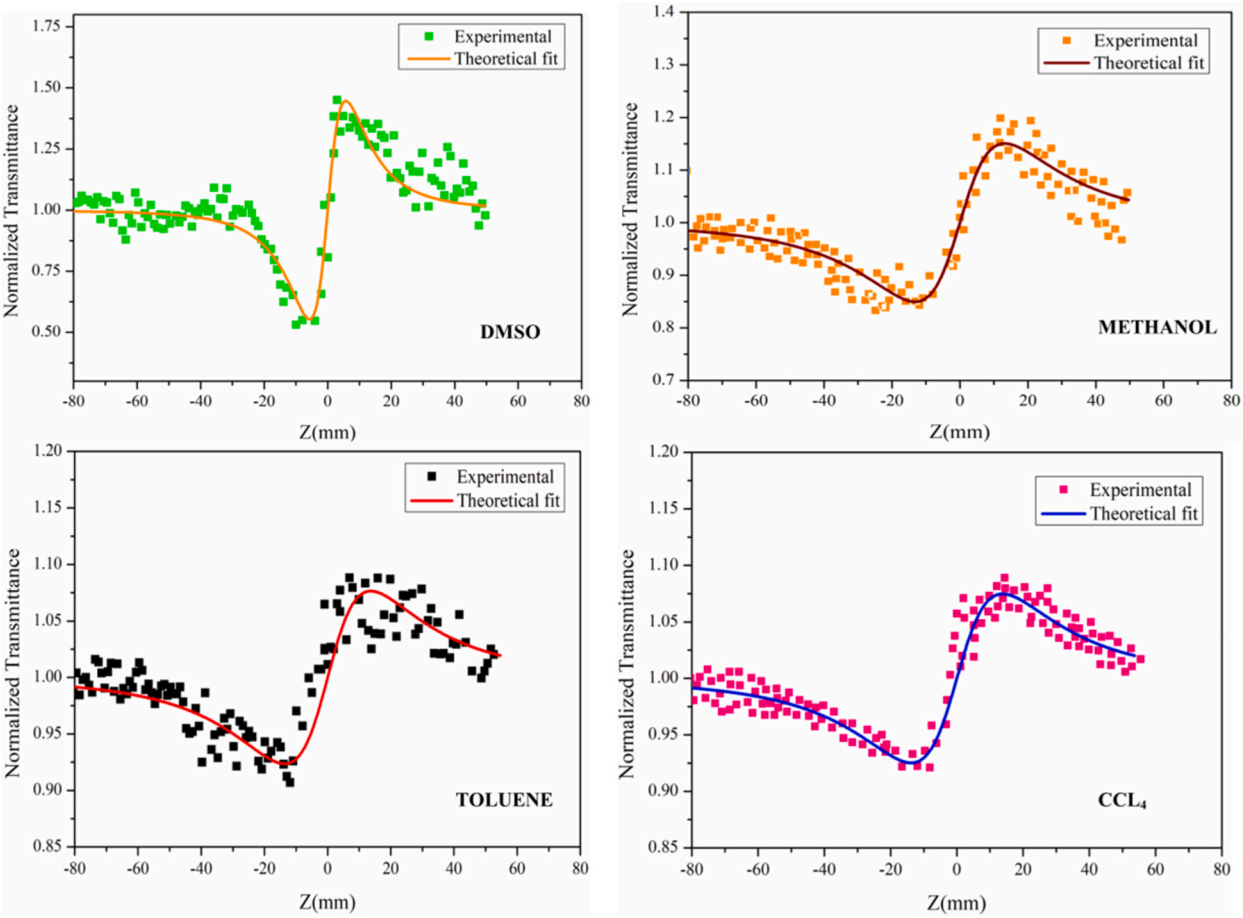

Fig. 5. CA Z-scan curves of 12D.

Table 2
Z-scan results 12D in four solvents.

	Solvent	β(× 10^{-12}) (m/W)	n_2 (× 10^{-19}) (m^2/W)	Re $\chi^{(3)}$ (×10^{-13}) (esu)	Im $\chi^{(3)}$ (× 10^{-13}) (esu)	$\chi^{(3)}$ (× 10^{-13}) (esu)	γ (*10^{-34}) (esu	
12D POLAR	DMSO	18.40	26.71	11.29	3.293	11.76	2.40	Present work
	METHANOL	17.35	9.03	3.54	2.88	4.56	1.07	
12D NONPOLAR	TOLUENE	3.63	4.57	1.97	0.66	2.07	0.41	
	CCl_4	2.56	4.47	1.98	0.48	2.04	0.38	
BFBD POLAR	DMSO	5.74	−5.54	−2.18	0.77	2.31	0.54	[34]
	METHANOL	8.43	−9.47	−9.63	3.63	10.29	0.29	
BFBD NONPOLAR	TOLUENE	1.67	−2.72	−1.19	0.31	1.23	0.23	
	CCl_4	3.45	−1.77	−1.49	1.23	1.9	0.09	

width, and, whereas the aforementioned parameters are not specified in computational method.

5.4.2. *Optical limiting (OL)*

Optical limiters are gaining popularity because of its ability to secure optically sensitive parts, optoelectronic components, and human eyes from powerful laser beams. Two-photon absorption (TPA), RSA, and nonlinear scattering are some nonlinear mechanisms that contribute to optical limiting (OL). RSA behaviour of materials with a positive NLA coefficient is evaluated by fair transmission at low intensities and a reduction in transmission at high intensity. The compound shows TPA mechanism that contributes to nonlinear absorption; hence it is appropriate for OL applications. The observed OL behaviour of 12D is shown in Fig. 6, which is a plot of input fluence (energy) vs. normalized transmittance using z-scan OA data. The threshold value describes a material's OL potential; low threshold value gives better optical limiting. Table 3 summarises the calculated OL threshold values for 12D in four solvents. The NLA coefficient is dependent on the polarity of the solvent employed, and the limiting threshold drops as the NLA coefficient rises. The limiting response can be tuned by changing the substitution on the phenyl rings.The outcome demonstrates that 12D has optical limiting behaviour in range 8.84–26.51 Jcm^{-2}, similar to the reported benzodiazepine derivative [34].

5.5. *UV–visible*

Fig. 7 depicts the absorption spectra of the 12D in DMSO, methanol, ethanol, toluene, and CCl_4. The TD-DFT approach was used to deduce the absorption spectra in five solvents. From the experimental spectra, the absorption wavelengths in DMSO are at 394 and 371 nm, in methanol at 344 nm, in ethanol at 346 nm, in toluene at 388 and 366 nm, and in CCl_4 at 377 and 328 nm. The bands at 534, 403, and 399 nm in DMSO, methanol, ethanol, and 524, 400 and 397 nm in toluene and CCl_4 are observed at TD-DFT calculation are shown in Table 4. This hypsochromic shift is brought on by the augmented solvation of the lone pair in the initial state, which is caused by the rising polarity of the solvents (DMSO > methanol > ethanol > toluene > CCl_4). The bands observed at 394, 346, 344, 388, and 377 nm in five solvents results from π → π* transitions and the intramolecular charge transfer (ICT) between amine group and nitrosubstituted phenyl ring and slightly near the bromophenyl ring; delocalization behavior of π electrons in the benzodiazepine moiety. The strong absorption in the range of 280–400 nm in methanol and ethanol is due to the presence of chromophores and auxochromes in the molecule. Chromophores are groups of atoms that are responsible for the colour of a molecule, and they have a delocalized system of electrons that can absorb light in the visible or ultraviolet range. In the case of methanol and ethanol, the chromophore responsible for this absorption is the carbonyl group (-CO) that is present in the molecule. Auxochromes are groups of atoms that can modify the intensity or wavelength of the absorption by interacting with the chromophore. In the case of methanol and ethanol, the hydroxyl

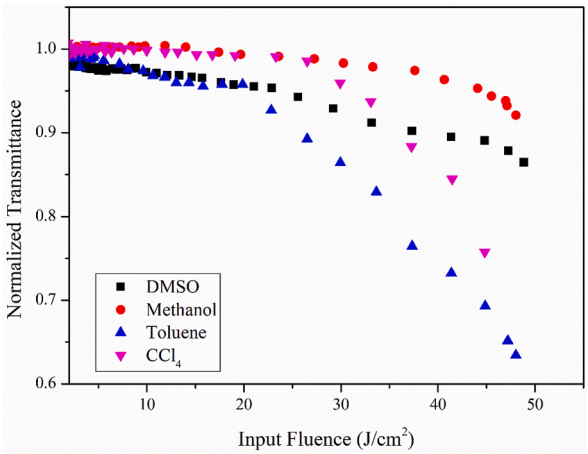

Fig. 6. Optical limiting curve of 12D.

Table 3
OL threshold values of 12D in four solvents.

Solvent	NLA Coefficient $\beta(\times 10^{-12})$ (m/W)	OLT(Jcm^{-2})
DMSO	18.40	8.84
METHANOL	17.35	14.003
TOLUENE	3.625	19.84
CCl_4	2.555	26.51

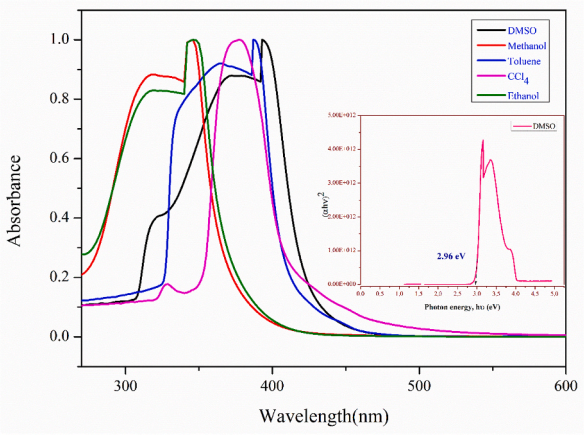

Fig. 7. UV–vis spectra of 12D.

Table 4
Excitation energies, absorption peaks and oscillator strength of 12D.

Solvent	Excitation	CI expansion coefficient	Wavelength(nm)		Energy(cm^{-1})	Oscillator Strength (f)
			Calculated	Experimental		
DMSO	H → L	0.70324	534.42		18712.05	0.0264
	H-1 → L	0.31744	403.75	394	24767.66	0.0862
	H → L+1	0.61921	399.01	371	25062.05	0.2283
Methanol	H → L	0.70328	534.23		18718.57	0.0254
	H-1 → L	0.63851	403.61	395	24776.53	0.0780
	H → L+1	0.63034	398.23		25111.25	0.2236
Toluene	H → L	0.70252	524.58		19062.9	0.0253
	H-1 → L	0.57527	400.88	388	24945.1	0.1131
	H → L+1	0.56717	397.06	366	25184.65	0.2259
CCL_4	H → L	0.70249	523.60		19097.59	0.0250
	H-1 → L	0.56941	400.46	377	24970.91	0.1145
	H → L+1	0.56123	396.58	328	25215.3	0.2201

group (-OH) is an auxochrome that can enhance the absorption of light by the carbonyl group. The combination of the carbonyl chromophore and the hydroxyl auxochrome in methanol and ethanol results in a strong absorption in the 280–400 nm range [47]. The protonation of imine nitrogen in the benzodiazepine ring can cause bathochromic shift in protic solvents. As the pH increases there is a slight blue shift in the absorption peak. However aprotic and nonpolar solvents might not affect the absorption maxima substantially [48]. Also NBO investigation supports the existence of CT interactions [49,50].

5.6. *Optical energy gap*

The feasibility of the compound for optoelectronic applications was identified by the band gap values from Tauc's plot. Materials with a small band gap will be more appropriate for NLO fabrication [46]. Tauc's relationship was employed to compute the optical energy gap of all substances.

$\alpha h\nu = \alpha_0(h\nu - E_g)^n$; where α_0 is a band tailing constant, E_g is the energy gap, and n is the transition mode's power factor [51]. The value of n is determined by the material's nature, as well as the photon transition. The optical E_g was calculated using the absorption spectrum by taking the value 2 for n, i.e for direct allowed transition. The data of UV–visible spectra was used to obtain the graph of

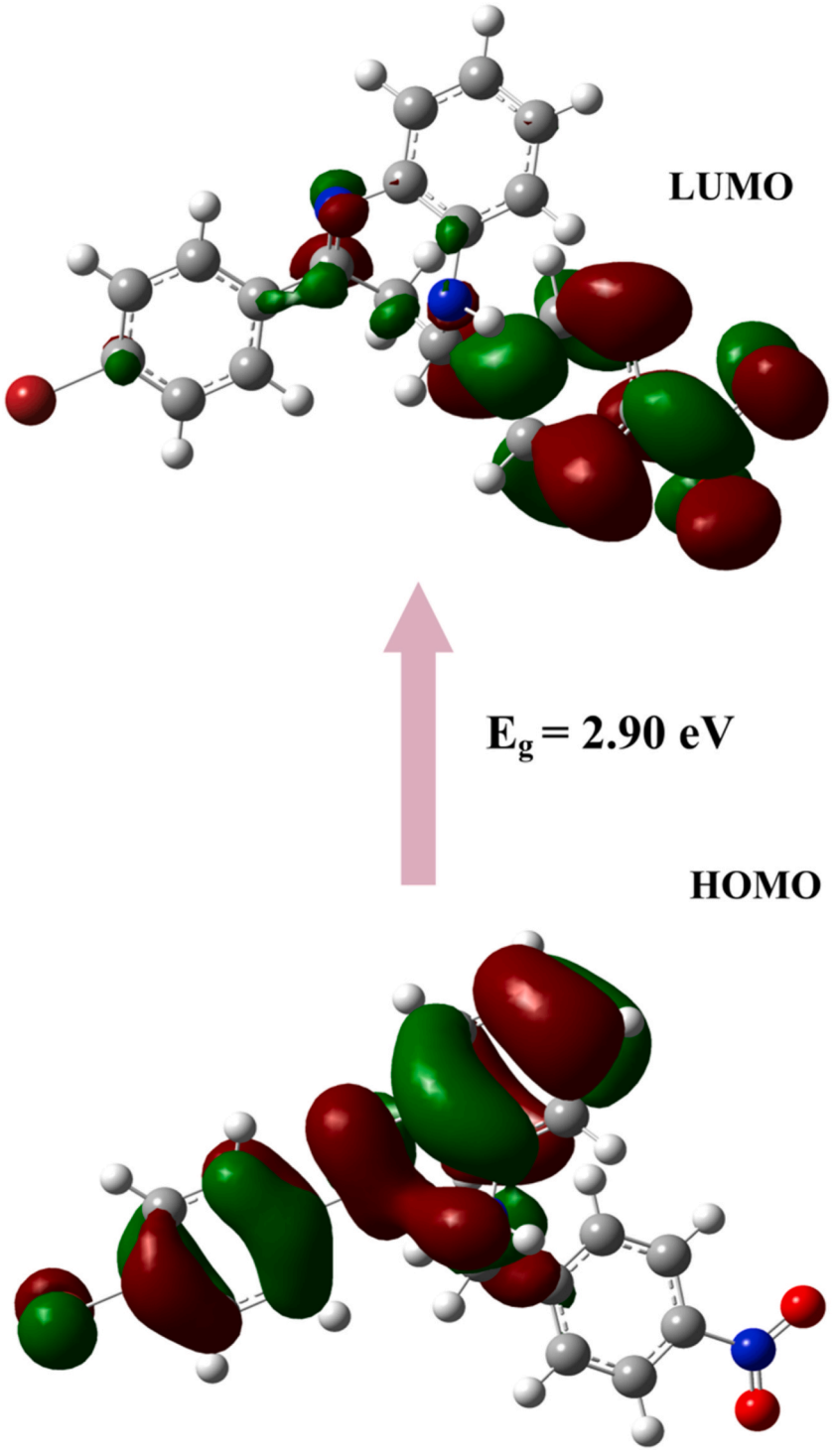

Fig. 8. HOMO-LUMO plot of 12D.

photon energy, E verses $(\alpha h\nu)^{2,}$ and the sloping straight line was extended and intersected at the X-axis to obtain the values of optical energy gap (E_g) and was found to be 2.96 eV.

5.7. Frontier molecular orbital analysis (FMO)

FMO yields prominent information that describes the electric charge transfer and optical response as well as the chemical activity [52]. The HOMO and LUMO energies calculated are −5.99 eV and −3.09 eV, respectively, and the E_g was computed to be 2.90 eV. In HOMO, electrons are located on benzodiazepine part and the bromophenyl ring is linked to this. In LUMO, the charge dissemination is over the nitrophenyl ring and the visual representation is shown in Fig. 8. This indicates that the CT takes place from benzodiazepine to nitrophenyl ring and the lowered energy gap confirms the third-order NLO response of the molecule. These results imply that the molecule exhibits good chemical strength and stability [53–56].

5.8. Fluorescence emission spectra

The fluorescence emission spectrum was recorded at an excitation of 350 nm, is given in Fig. 9. The prominent emissions are seen at 400 nm–460 nm in four solvent conditions, indicating that 12D emits blue fluorescence and could be used to fabricate blue light emitting diodes (LEDs). Strong intramolecular CT interactions cause the broad spectral characteristics seen in DMSO solvent [57]. The emergence of ICT states is one of the key explanations for the fluorescence effect. The CT interaction between the nitro and bromo phenyl group with the amine group via π -conjugated system is well explained by the ICT from donor to acceptor, modifying the dipole moment [20]. When a molecule moves from its initial state into its excited state, the electron cloud drive on D-A might cause it to become heavily polarized [58]. The luminescent emission spectra of a molecule can provide information about its electronic structure, molecular symmetry, and the interactions between the molecule and the surrounding solvent molecules. The electronic structure of the molecule can strongly influence the emission spectra. For example, the position of the excited state energy levels, the symmetry of the molecule, and the nature of the excited state can all affect the emission spectra. A change in the molecular structure, such as the addition of a functional group, can result in a shift in the emission wavelength or intensity. The polarity of the solvent can also have a significant impact on the emission spectra. In polar solvents, the excited state of the molecule may interact more strongly with the surrounding solvent molecules, leading to a shift in the emission wavelength or intensity. Conversely, in nonpolar solvents, the excited state of the molecule may be less affected by the solvent, resulting in a different emission spectrum. The interactions between the solvent molecules can also affect the emission spectra. In a strongly interacting solvent environment, such as a hydrogen-bonded network, the molecule may experience a different electronic environment than in a non-interacting solvent. This can result in a shift in the emission wavelength or intensity. In general, the luminescent emission spectra of a molecule can be influenced by the molecular structure and the interaction between the molecule and the surrounding solvent molecules [59,60].

5.9. Natural bond orbital analysis

NBO analysis investigates how filled π orbitals (donors) interact with vacant anti-bonding orbitals (acceptors). The charge transfer

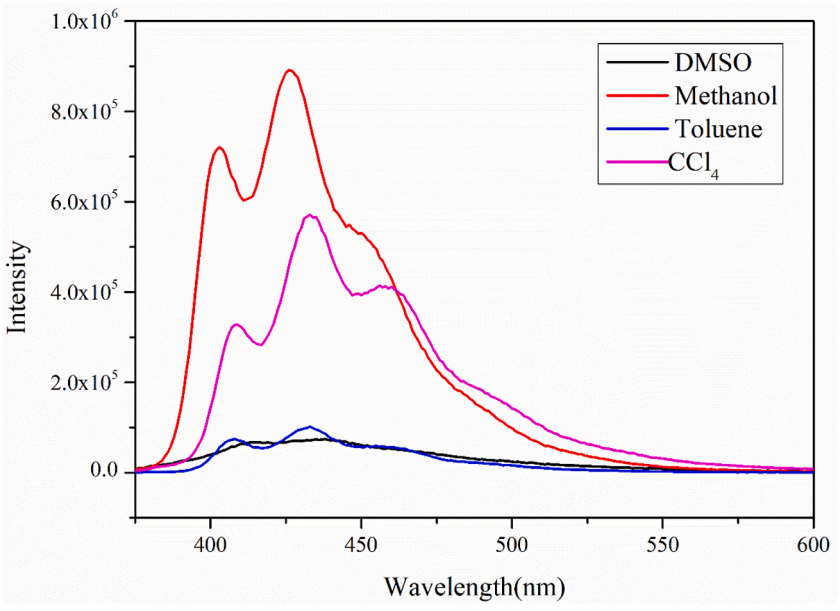

Fig. 9. Emission spectra of 12D under 350 nm excitation.

interactions within the molecule is revealed by NBO analysis and was performed using the NBO 3.1 program. Large E(2) values are used to examine the intense interaction between D-A and the system's conjugation [61,62]. The effective CT link between LP N8 → π* (C1–C2) gives an energy of 22.25 kcal/mol due to the nitrogen atom attached to the benzodiazepine ring. The intramolecular hyper-conjugative interaction between LP (1) N8 → σ* (C13–C17) and LP (1) N8 → σ* (C13–H18) show an energy value of 5.91 and 4.97 kcal/mol, respectively. The interaction energy of π (C17–C36) → π* (C34–C35) and π (C21–C22) → π* (C34–C35) are higher (23.83 kcal/mol & 15.93 kcal/mol respectively) suggests the electron delocalization behaviour of nitrogen atoms in the diazepine ring. The hyperconjugation σ (N8–H16) → σ* (C2–C3), σ (C13–H18) → σ* (C17–C32), σ (C14–H20) → σ* (N9–C15), and σ (C22–C23) → σ* (C24–Br29) show stabilization energies of 4.08, 4.58, 4.40 and 5.57 kcal/mol respectively. These results show that an ICT takes place in the molecule from the benzodiazepine and bromophenyl ring to the nitrophenyl ring. These intramolecular interactions enhance stability, which strengthens the NLO behaviour of the molecule.

5.10. Natural population analysis

The atomic charge dissemination over the bonds is studied using natural population analysis (NPA). Atomic charges on each atom affect a molecule's electronic structure, polarizability, and electrochemical characteristics. The generation of D-A pairs and CT takes place inside the molecule as a result of the spread of charges over the atoms, which improves the molecule's NLO response [63]. Fig. 10 depicts a plot of atomic charges. The natural charge of the nitrogen N39 (0.48494 e) atom is more positive than other atoms as a result of the direct bonding of O43 and O42 oxygen atoms. From the entire hydrogen atoms, H16 (0.37279 e) shows the highest positive charge than others owing to the direct linkage of the nitrogen atom in the diazepine ring. The N8 (−0.63327 e) and N9 (−0.45285 e) nitrogen atoms are negatively charged which is confirmed by the formation of C14–H19···N8 and C4–H10···N9 hydrogen bonding. Even though electronegative atoms attract electrons, the carbon atoms bonded to the nitrogen atoms C2, C3, C15, and C34 are more positive.

5.11. Molecular Electrostatic Potential (MEP)

MEP is frequently employed as a reactivity map to show obvious sites having electrophilic nature on an organic molecule [64]. It is correlated to electron density and offers an observable way to interpret a molecule's relative polarity and explain hydrogen bonding, [65–67]. Electrostatic potential (EP) is represented by three colours: red for the lowest potential, blue the highest potential, and green for zero.

The protons are attracted to the aggregate electron density in the molecule (represented by negative EP- red shade), while the atomic nuclei repel them (represented by positive EP- blue shade). The EP surfaces are taken to picture the reactive sites for nucleophilic and electrophilic areas, as illustrated in Fig. 11. Nucleophilic reactivity is depicted by the positive (blue) while electrophilic attack is represented by the negative (red) regions. The nucleophilic reactivity of the compound is primarily centered on the nitrogen in the benzodiazepine region and slightly near the bromophenyl area. At the same time, the red region is primarily isolated on the O42 and O43 atoms in the nitrophenyl ring.

5.12. Vibrational analysis

Identification of vibrational modes were performed using experimental Raman and IR spectra, normal coordinate analysis (NCA), Gaussian force field computations, and scaled quantum mechanical force field (SQMFF) approach with PED data. The SQMFF technique is vital for reducing systematic errors caused by mechanical anharmonicity. The selective scaling approach is used following NCA to compensate for shortcomings and to complement the computed vibrational frequencies to the experimentally obtained. The molecule has 43 atoms, producing 123 normal modes. It comes under the C1 point group since the molecular conformation obtained during geometry optimization has no particular symmetries. Figs. 12 and 13 illustrate the FT-IR and FT-Raman spectra. The experimental and simulated FT-IR and FT-Raman band assignments are shown in Table 5. The slight deviation of simulated results from the experimental values are due to the fact that the simulated results are from isolated molecule in gas phase while the experimental results are from solid phase.

N–H stretching wavenumber for the diazepine ring is predicted to be in the range of 3300–3500 cm^{-1} [68]. N–H stretching is attributed to a strong band with a PED of 100% in the IR spectra at 3516 cm^{-1}. The N–H in-plane bending mode (PED 32%) is attributed to the band at 1396 cm^{-1} in the infrared and 1182 cm^{-1} in Raman. Having a PED of 52%, the N–H out-of-plane bending mode is the one ascribed to the Raman band at 409 cm^{-1}. Intermolecular N–H• • •N hydrogen bonding blue shifts the N–H stretching wavenumber and red shifts the N–H bending wavenumber. The range of 3100-3000 cm^{-1} is often where the aromatic C–H stretching vibrations are detected [69]. The C–H stretching vibration is detected at 3001 cm^{-1} in the infrared and has a computed value of 3052 cm^{-1} with a PED of 98%. C═C, C–C, and C–N stretching modes are associated with the C–H in plane bending vibration. IR active C–H in-plane bending modes are seen at 1549 cm^{-1}, 1491 cm^{-1}, and 1423 cm^{-1} with PED 30%.

The vibrations of $–NO_2$ group exhibit substantial absorption in the ranges of 1570-1485 cm^{-1} and 1370-1320 cm^{-1}, respectively [70]. The bands at 1598 cm^{-1} in Raman and 1549 cm^{-1} in IR are responsible for the unsymmetrical stretching vibration, the band at 1348 cm^{-1} in Raman is found within the expected range of symmetric stretching band. C–N stretching, whose anticipated area is 1180-865 cm^{-1}, is what causes the observed Raman bands at 1195 cm^{-1} [71,72]. The $–NO_2$ group is predicted to exhibit in-plane bending vibrations in the 590–500 cm^{-1} range. The bands were seen at 635 cm^{-1} in IR and Raman, and 534 cm^{-1} in Raman, ascribed to $–NO_2$ in-plane-bending mode. Due to C–Br stretching vibrations, usually, aromatic bromo compounds absorb substantially

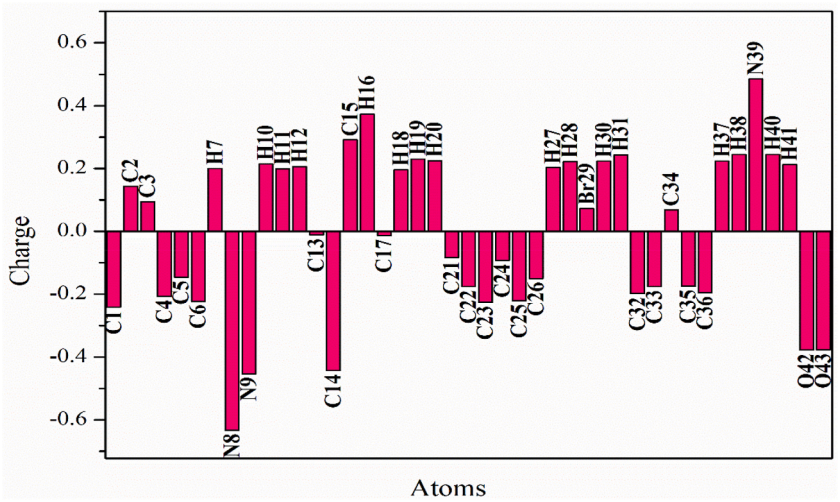

Fig. 10. Atomic charge distribution plot of 12D.

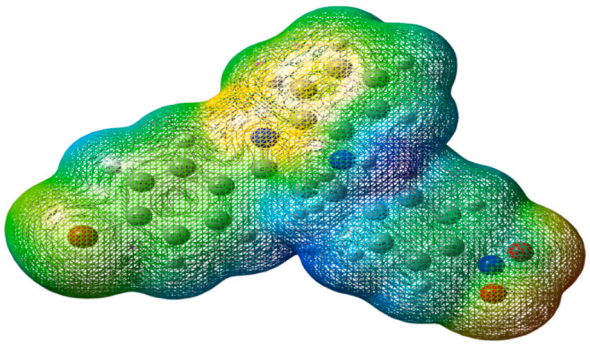

Fig. 11. Molecular Electrostatic Potential surface map of 12D.

in the range of 650-395 cm^{-1} [73]. In Raman and IR, the C–Br stretching mode for 12D is assigned at 635 cm^{-1} with a PED of 18%. The concurrent IR and Raman activity of the Bromo and Nitro phenyl ring vibrations offer confirmation for the charge transfer (CT) between the D-A groups, which leaves the molecule thoroughly polarised, and this intramolecular CT (ICT) interaction governs the NLO response of the molecule [74].

6. Conclusion

Combined theoretical and experimental investigation on the third-order NLO response of the title compound has been carried out. Different spectroscopic methods; FT-Raman, FT-IR, UV–Visible, and Z-scan technique, along with the computational DFT method, were used to analyze the structural, linear, and NLO properties of the title compound. The HOMO- LUMO and NBO analyses reveal the intramolecular charge transfer interactions. The HOMO-LUMO energy gap calculated using TD-DFT was confirmed with the experimental energy gap using Tauc plot. The first and second-order hyperpolarizability computation results reveal the NLO response of the molecule. From OA and CA z- scan measurements, the 2 PA behaviour is evident with a positive NLR index. NLA coefficient β (m/w), the NLR index n_2 (m^2/w), and the third-order NLO susceptibility $\chi^{(3)}$ (esu) are in the order of 10^{-12}, 10^{-19} and 10^{-13} respectively. The γ value is of the order of 10^{-34} esu in experimental as well as theoretical analysis. These third-order nonlinear parameters show that the compound has a substantial NLO response and could be used in Optical limiting applications such as optical sensors and photodetector protection.

Author contribution statement

P.ASWATHY- Performed the experiments, Analyzed and interpreted the data, Wrote the paper.
I. HUBERT JOE - Conceived and designed the experiments.
B.NARAYANA - Analyzed and interpreted the data.
B.K. SAROJINI; K.R HARSHITHA; J. CLEMY MONICKA - Contributed reagents, materials, analysis tools or data.

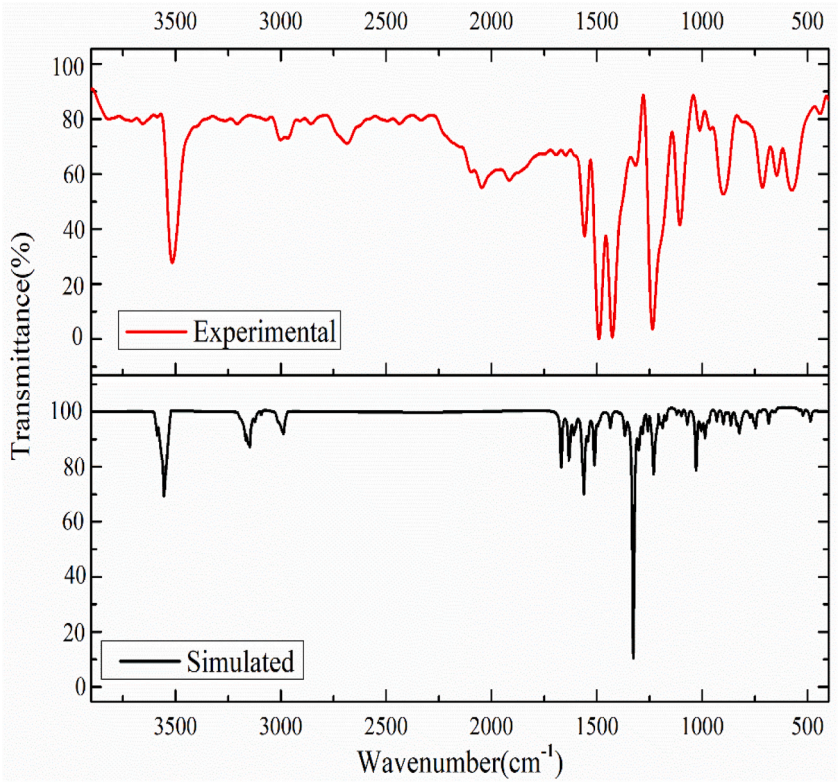

Fig. 12. FT-IR spectra of 12D.

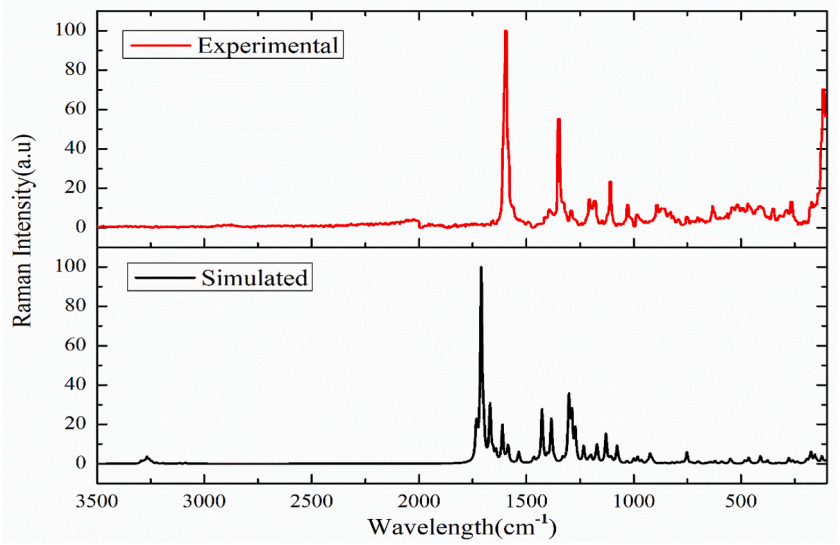

Fig. 13. FT-Raman spectra of 12D.

Table 5
Experimental and Simulated vibrational band assignment of 12D.

Calculated Wavenumber(cm^{-1})		Experimental Wavenumber(cm^{-1})		Assignment with PED (%)
Unscaled	Scaled	IR	Raman	
3577	3516	3516	–	ν N_8–H_{16}(100)
3221	3153	–	–	ν Ph1 C_1–H_7(92), ν Ph2 C_{22}–H_{27}(80), ν Ph3 C_{33}–H_{38}(76) + νPh3 C_{35}–H_{40}(77)
3121	3052	3001	–	ν Ph3 C_{36}–H_{41}(98), ν C_{13}–H_{18}(94), ν_{as} C_{14}–H_{19}(90)+ ν_{as} C_{14}–H_{20}(86)
1660	1628	–	1598	ν N_9═C_{15}(21), ν_{as} N_{39}–O_{42}(16)+ ν_{as} N_{39}–O_{43}(16)
1578	1528	1549		$\nu_{as}N_{39}$-O_{42}(24)+ $\nu_{as}N_{39}$-O_{43}(24), ν Ph2 C_{23}═C_{24}(18), ν N_9═C_{15}(22), δ_{sci} $CH_{2\ (H19-C14-H20)}$ (19)
1518	1508	1491	–	δ_{in} Ph3C_{36}–C_{35}–H_{40} (10), δ_{in} Ph3C_{32}–C_{33}–H_{38} (10)
1422	1395	1423	–	ν Ph2 C25═C26(16), ν Ph2 C22–C23(14), δ_{in} C_2–N_8–H_{16}(10) δ_{in} Ph2C_{24}–C_{23}–H_{28} (10), δ_{in} Ph2C_{21}–C_{26}–H_{31} (8)
1369	1553	–	1348	ν_{as} N_{39}–$O_{43,42}$(32), δ_{wag} C14–C13–H18 (15), δ_{in} C13–C14–H19(8), ν $_{skele}$ C13–C14(8)
1324	1279	1297	1290	ν C_1–C_6(42), δ_{in} Ph2 C_{21}–C_{22}–H_{27}(12)
1290	1242	1228	–	ν Ph2 C_{23}–C_{24}(25), ν Ph2 C_{24}–C_{25}(23),
1260	1189	–	1195	ν C_2–N_8(26), ν C_3–N_9(25), ν C_{15}–C_{21}(18), δ_{in} Ph2 C_{22}–C_{23}–H_{28} (20)
1197	1131	–	1114	ν $_{skele}$ C_{13}–C_{17}(34), ν Ph3 C_{32}–C_{33}(18), + δ_{in} Ph3 C_{32}–C_{33}–H_{38}(12)
1118	1057	1092	–	ν N_8–C_{13}(25), ν N_{39}–C_{34}(26), δ_{out} Ph3C36–C35–H40 (7)
1087	1029	–	1025	τ H_{37}–C_{32}–C_{33}–H_{38}(28), ν Ph2 C_{23}═C_{24}(14), ν Ph2 C_{24}–C_{25} (14)
1031	980	997	–	τ H_{30}–C_{25}–C_{26}–H_{31}(30), τ H_{10}–C_4–C_5–H_{11}(16) τ H_{11}–C_5–C_6–H_{12}(16), τ OOPB C_{21}–C_{26}–C_{25}–H_{31}(7), τ OOPB C_{17}–C_{32}–C_{33}–H_{37}(5)
1019	969	–	991	τ H_{40}–C_{35}–C_{36}–H_{41}(18), τ C_{33}–C_{34}–N_{39}–O_{43}(6)
887	889	887	887	ν $_{skele}$ N_8–C_{13} (26), τ C_3–C_2–N_8–H_{16}(14)
759	714	708	–	ν C_{13}–C_{17}(21), τ C_{33}–C_{34}–N_{39}–O_{43}(20)
704	643	635	635	τ C_{33}–C_{34}–N_{39}–O_{43}+ τ C_{33}–C_{34}–N_{39}–O_{42}(40), ν Ph3 C_{24}–Br_{29}(18),
601	557	561	–	δ_{in} C_{34}–C_{35}–C_{36}(13), δ_{in} C_{32}–C_{33}–C_{34}(13)
559	511	–	534	δ_{def} C_{34}–N_{39}–O_{43}(36)+ δ_{def} C_{34}–N_{39}–O_{43}(33)
545	450	–	460	τ C_{35}–C_{34}–N_{39}–O_{43}(14), τ C_{17}–C_{36}–C_{35}–C_{34}(10)
506	447	–	411	δ_{def} C_{15}–C_{21}–C_{26}(16), τ C_{21}–C_{22}–C_{23}–C_{24} (15)
420	335	–	351	τ C_{17}–C_{32}–C_{33}–C_{34} (19)
361	269	–	271	δ_{in} C_{33}–C_{34}–N_{39} (19), δ C_{33}–C_{24}–Br_{29}(15), δ C_{25}–C_{24}–Br_{29}(11)

ν –stretching, p-Ph1 –paradisubsitited phenyl ring 1, p-Ph2 –paradisubsitited phenyl ring 2, o-Ph3 –orthodisubsitited phenyl ring3, δ_{in} –in-plane bending, δ_{out} –out-of plane bending, δ_{sci} –scissoring, δ_{wag} –wagging, ν $_{skele}$ –skeletal stretching, breath –breathing, τ –torsion, OOPB- out-of plane bending.

Additional information

No additional information is available for this paper.

Declaration of competing interest

The authors declare that they have no known competing financial interests or personal relationships that could have appeared to influence the work reported in this paper.

References

[1] Y. Zhao Y, Z. Li, Q. Li, Q.Y. Zhao, R. Yao, C. Ma, Y. Zhang, D. Wang, Optical properties of new third-order nonlinear materials modified by click chemistry, Molecules 27 (15) (2022) 5006, https://doi.org/10.3390/molecules27155006.
[2] B. Liang, J. Zhao, J. Wang, J.Y. Li, B. Han, J. Li, J.X. Ding, Z. Xie, H. Wang, S. Zhou, Nonlinear optical properties of porphyrin-based covalent organic frameworks determined by steric-orientation of conjugation, J. Mater. Chem. C 11 (9) (2023) 3354–3359, https://doi.org/10.1039/D2TC05258J.
[3] M. Sabbaghan, M. Nadafan, M, V.J. Ahmadi, The effect of aromatic and non-aromatic ionic liquids on the optical nonlinearity responses of porphyrins, J. Mol. Liq. 348 (2022), 118398, https://doi.org/10.1016/j.molliq.2021.118398.
[4] V. Turchenko, A. Trukhanov, S. Trukhanov, M. Balasoiu, N. Lupu, Correlation of crystalline and magnetic structures of barium ferrites with dual ferroic properties, J. Magn. Magn Mater. 477 (2019) 9–16, https://doi.org/10.1016/j.jmmm.2018.12.101.

[5] M.V. Zdorovets, A.L. Kozlovskiy, D.I. Shlimas, D.B. Borgekov, Phase transformations in FeCo - Fe2CoO4/Co3O4-spinel nanostructures as a result of thermal annealing and their practical application, J. Mater. Sci. Mater. Electron. 32 (2021) 16694–16705, https://doi.org/10.1007/s10854-021-06226-5.

[6] P.N. Prasad, D.J. Williams, Introduction to Nonlinear Optical Effects in Molecules and Polymers, second ed., Wiley, New York, 1992.

[7] A.V. Trukhanov, N.A. Algarou, Y. Slimani, M.A. Almessiere, A. Baykal, D.I. Tishkevich, D.A. Vinnik, M.G. Vakhitov, D.S. Klygach, M.V. Silibin, T.I. Zubar, S. V. Trukhanov, Peculiarities of the microwave properties of hard-soft functional composites SrTb0.01Tm0.01Fe11.98O19-AFe2O4 (A = Co, Ni, Zn, Cu and Mn), RSC Adv. 10 (2020), 32638, https://doi.org/10.1039/d0ra05087c.

[8] A.L. Kozlovskiy, M.V. Zdorovets, Effect of doping of Ce4+/3+ on optical, strength and shielding properties of (0.5-x)TeO2-0.25MoO-0.25Bi2O3-xCeO2 glasses, Mater. Chem. Phys. 263 (2021), 124444, https://doi.org/10.1016/j.matchemphys.2021.124444.

[9] S. Shettigar, P. Poornesh, G. Umesh, B.K. Sarojini, B. Narayana, K.P. Kamath, Investigation of third-order nonlinear optical properties of conjugated benzodioxal derivatives, Opt Laser. Technol. 42 (2010) 1162–1166, https://doi.org/10.1016/j.optlastec.2010.03.002.

[10] P. Poornesh, S. Shettigar, G. Umesh, K.B. Manjunatha, K.P. Kamath, B.K. Sarojini, B. Narayana, Nonlinear optical studies on 1,3-disubstituent chalcones doped polymer films, Opt. Mater. 31 (2009) 854–859, https://doi.org/10.1016/j.optmat.2008.09.007.

[11] P. Poornesh, K. Ravi, G. Umesh, P.K. Hegde, M.G. Manjunatha, K.B. Manjunatha, A.V. Adhikari, 3,3′-Benzene-1,4-diylbis[1-(substituted)phenylprop-2-en-1-one] derivatives: a new class of materials for third-order nonlinear optical applications, Opt Commun. 283 (2010) 1519–1527, https://doi.org/10.1016/j.optcom.2009.12.015.

[12] K. Janardhana, V. Ravindrachary, P.C. Rajesh Kumar, Ismayil Yogisha, Third order nonlinear optical studies of 1-(4-chloro phenyl)-3-(4- dimethylamino phenyl) prop- 2-en-1-one, J. Cryst. Growth 368 (2013) 11–20, https://doi.org/10.1016/j.jcrysgro.2012.12.169.

[13] L. Kamath, K.B. Manjunatha, S. Shettigar, G. Umesh, B. Narayana, S. Samshuddin, B.K. Sarojini, Investigation of third-order nonlinear and optical power limiting properties of terphenyl derivatives, Opt Laser. Technol. 56 (2014) 425–429, https://doi.org/10.1016/j.optlastec.2013.09.025.

[14] H.J. Ravindra, A. John Kiran, K. Chandrasekharan, H.D. Shashikala, S.M. Dharmaprakash, Third order nonlinear optical properties and optical limiting in donor/acceptor substituted 4′-methoxy chalcone derivatives, Appl. Phys. B 88 (2007) 105–110, https://doi.org/10.1007/s00340-007-2677-8.

[15] M. Shkir, P.S. Patil, M. Arora, S. AlFaify, H. Algarni, An experimental and theoretical study on a novel donor-π-acceptor bridge type 2, 4, 5-trimethoxy-4′-chlorochalcone for optoelectronic applications: a dual approach, Spectrochim. Acta Part A: Mol. Biomol.Spectrosc 173 (2017) 445–456, https://doi.org/10.1016/j.saa.2016.09.022.

[16] B.A. Reinhardt, L.L. Brott, S.J. Clarson, A.G. Dillard, J.C. Bhatt, R. Kannan, L. Yuan, S. Guang, P.N. Prasad, Highly active two-photon dyes: design, synthesis, and characterization toward application, Chem. Mater. 10 (1998) 1863–1874, https://doi.org/10.1021/cm980036e.

[17] M. Albota, D. Beljonne, J.L. Bredas, J.E. Ehrlich, J.Y. Fu, A.A. Heikal, S.E. Hess, T. Kogej, M.D. Levin, S.R. Marder, D.M. Maughon, J.W. Perry, H. Rockel, M. Rumi, G. Subramaniam, W.W. Webb, X.L. Wu, C. Xu, Design of organic molecules with large two-photon absorption cross sections, Science 281 (1998) 1653–1656, https://doi.org/10.1126/science.281.5383.1653.

[18] B. Rajashekar, P. Sowmendran, S. Sai, G.N. Rao, Synthesis, characterization and two-photon absorption based broadband optical limiting in diarylideneacetone derivative, J. Photochem. Photobiol., A: Chem 238 (2012) 20–23, https://doi.org/10.1016/j.jphotochem.2012.04.006.

[19] S. Muthu, M. Prasath, R.A. Balaji, Experimental and theoretical investigations of spectroscopic properties of 8-chloro-1-methyl-6-phenyl-4H [1, 2, 4] triazolo [4, 3-a][1, 4] benzodiazepine, Spectrochim, Acta, Part A 106 (2016) 129–145, https://doi.org/10.1016/j.saa.2012.12.057.

[20] M. Prasath, S. Muthu, R.A. Balaji, Vibrational spectroscopy investigation using ab initio and DFT vibrational analysis of 7-chloro-2-methylamino-5-phenyl-3H-1,4- benzodiazepine-4-oxide, Spectrochim. Acta, Part A 113 (2013) 224–235, https://doi.org/10.1016/j.saa.2013.04.104.

[21] S. Muthu, M. Prasath, E.I. Paulraj, R.A. Balaji, " FT-IR, FT-Raman spectra and ab initio HF and DFT calculations of 7-chloro -5- (2-chlorophenyl) -3-hydroxy-2, 3-dihydro-1H-1, 4-benzodiazepin-2-one", Spectrochim. Acta, Part A 120 (2014) 185–194, https://doi.org/10.1016/j.saa.2013.09.150.

[22] B.P. Ngoy, A.K. May, J. Mack, T. Nyokong, Effect of bromination on the optical limiting properties at 532 nm of BODIPY dyes with p-benzyloxystyryl groups at the 3,5- positions, J. Mol. Struct. 1175 (2019) 745–753, https://doi.org/10.1016/j.molstruc.2018.08.012.

[23] J. Harris, L. Gai, G. Kubheka, J. Mack, T. Nyokong, Z. Shen, "Optical limiting properties of 3,5-dithienylenevinylene BODIPY dyes at 532 nm,", Chem. Eur J. 23 (2017) 14507–14514, https://doi.org/10.1002/chem.201702503.

[24] G. Kubheka, O. Achadu, J. Mack, T. Nyokong, Optical limiting properties of 3,5- diphenyldibenzo-azaBODIPY at 532 nm, New J. Chem. 41 (2017) 12319–12325, https://doi.org/10.1039/C7NJ01503H, 2017.

[25] M. Shkir, P.S. Patil, M. Arora, S. AlFaify, H. Algarni, An experimental and theoretical study on a novel donor-π-acceptor bridge type 2, 4, 5-trimethoxy-4'-chlorochalcone for optoelectronic applications: a dual approach, Spectrochim. Acta Mol. Biomol. Spectrosc. 173 (2017) 445–456, https://doi.org/10.1016/j.saa.2016.09.022.

[26] K. Janardhana, V. Ravindrachary, P.C. Rajesh Kumar, Ismayil Yogisha, Third order nonlinear optical studies of 1-(4-chloro phenyl)-3-(4- dimethylamino phenyl) prop- 2-en-1-one, J. Cryst. Growth 368 (2013) 11–20, https://doi.org/10.1016/j.jcrysgro.2012.12.169.

[27] E. Mathew, V.V. Salian, B. Narayana, I.H. Joe, Experimental and theoretical approach on third-order optical nonlinearity of a highly efficient anthracene-based chalcone derivative for optical power limiting, J. Mol. Struct. 1250 (2022), 131704, https://doi.org/10.1016/j.molstruc.2021.131704.

[28] A.D. Becke, Density- functional thermochemistry. III. The role of exact exchange, J Chem. Phy 98 (1993) 5648–5652, https://doi.org/10.1063/1.464913.

[29] A.D. Becke, Density-functional exchange-energy approximation with correct asymptotic behaviour, Phys. Rev. A. 38 (1988) 3098–3100, https://doi.org/10.1103/physreva.38.3098.

[30] T. Sundius, Molvib - a flexible program for force field calculations, J. Mol. Struct. 218 (1990) 321–326. T. Sundius, Molvib - a flexible program for force field calculations, J. Mol. Struct. 218 (1990) 321–326.

[31] T. Sundius, Scaling of ab initio force fields by MOLVIB, Vib. Spectrosc. 29 (2002) 89–95, https://doi.org/10.1016/S0924-2031(01)00189-8.

[32] Z. Baktır, M. Akkurt, S. Samshuddin, B. Narayana, H.S. Yathirajanc, 2, 4- bis(4-fluorophenyl)-2,3-dihydro-1H-1,5-benzodiazepine, Acta Cryst E67 (2011) o1262–o1263, https://doi.org/10.1107/S1600536811015455.

[33] D.A. Kleinman, Nonlinear dielectric polarization in optical media, Phys. Rev. 126 (1962) 1977–1979, https://doi.org/10.1103/PhysRev.126.1977.

[34] P. Aswathy, I.H. Joe, S. Samshuddin, B. Narayana, J.C. Monicka, Third-order NLO studies of 2, 4-Bis (4-fluorophenyl)-2, 3-dihydro-1H-1, 5-benzodiazepine using Z-scan technique and DFT method, J. Mol. Struct. 1246 (2021 Dec 15), 131169, https://doi.org/10.1016/j.molstruc.2021.131169.

[35] M. Sheik-bahae, A.A. Said, E.W. Van Stryland, High-sensitivity, single-beam n 2 measurements, Opt. Lett. 14 (1989) 955–957.

[36] M. Sheik-Bahae, A.A. Said, T. Wei, D.J. Hagan, E.W. Van Stryland, Sensitive mea- surement of optical nonlinearities using a single beam, IEEE J. Quantum Electron 26 (1990) 760–769, https://doi.org/10.1109/3.53394.

[37] X. Tian, R. Wei, Q. Guo, Y. Zhao, J. Qiu, Reverse saturable absorption induced by phonon-assistedanti-Stokes processes, Adv. Mater. (2018), 1801638, https://doi.org/10.1002/adma.201801638.

[38] Y. Chen, T. Bai, N. Dong, F. Fan, S. Zhang, X. Zhuang, J. Sun, B. Zhang, X. Zhang, J. Wang, W.J. Blau, Graphene and its derivatives for laser protection, Prog. Mater. Sci. 84 (2016) 118, https://doi.org/10.1016/j.pmatsci.2016.09.003.

[39] S. Valligatla, K.K. Haldar, A. Patra, N.R. Desai, Nonlinear optical switching and optical limiting in colloidal CdSe quantum dots investigated by nanosecond Z-scan measurement, Opt Laser. Technol. 84 (2016) 87–93, https://doi.org/10.1016/j.optlastec.2016.05.009.

[40] R. Kumar, A. Kumar, N. Verma, R. Philip, B. Sahoo, FeCoCr alloy-nanoparticle embedded bamboo-type carbon nanotubes for non-linear optical limiting application, J. Alloys Compd. 849 (2020), 156665, https://doi.org/10.1016/j.jallcom.2020.156665.

[41] Pieter NeethlingDetermining Nonlinear Optical Properties Using Z-Scan Technique, University of Stellenbosch, South Africa, 2005.

[42] T. Cassano, R. Tommasi, M. Ferrara, F. Babudrı, G.M. Farinola, F. Naso, Substituent-dependence of the optical nonlinearities m poly 2,5-dialkoxy-p-phenylenevinylene) polymers investigated by the 2-scan technique, Chem. Phys. 272 (2001) 111–118, https://doi.org/10.1016/S0301-0104(01)00453-0.

[43] B. Derkowska-Zielinska, M. Barwiolek, C. Cassagne, G. Boudebs, Nonlinear optical study of Schiff bases using Z-scan technique, Opt Laser. Technol. 124 (2020 Apr 1), 105968, https://doi.org/10.1016/j.optlastec.2019.105968.

[44] J. Kabatc, B. Jędrzejewska, P. Orliński, J. Pączkowski, The synthesis and the solvent and substituent effect on the spectroscopic characteristic of 3-ethyl-2-(p-substitued styryl) benzothiazolium iodides, Spectrochim. Acta A Mol. 62 (1–3) (2005 Nov 1) 115–125, https://doi.org/10.1016/j.saa.2004.12.014.

[45] A.M. Arif, A. Yousaf, H.L. Xu, Z.M. Su, Spectroscopic behavior, FMO, NLO and substitution effect of 2-(1H-Benzo [d] imidazole-2-ylthio)-No-substituted-acetamides: experimental and theoretical approach, Dyes Pigm 171 (2019 Dec 1), 107742, https://doi.org/10.1016/j.dyepig.2019.107742.

[46] P. Rosalyn, P. Kannan, G. Vinitha, A. Ramalingam, Effect of halogen substitution on azo-naphthol dye based poly (alkyloxymethacrylate) s and their Z-scan measurements, J. Mater. Sci. Mater. Electron. 20 (9) (2009 Sep) 835–843, https://doi.org/10.1007/s10854-008-9803-1.

[47] M.S. H Akash, K. Rehman, Ultraviolet-visible (UV-VIS) Spectroscopy, Essentials of pharmaceutical analysis, 2020, pp. 29–56, https://doi.org/10.1007/978-981-15-1547-7_3.

[48] M.M. Orive, B. Gallo, R.M. Alonso, F. Vicente, J.C. Viré, G.J. Patriarche, Spectrophotometric study of the acid-base equilibria of an imidazobenzodiazepine, midazolam, and its determination in pharmaceutical formulations, Mikrochim. Acta 97 (1989) 181–190, https://doi.org/10.1007/BF01242464.

[49] A.S. Akinyeye, S. Banjo, A.A. Idowu, Quantum-chemical and solvatochromic analysis of solvent effects on the electronic absorption spectra of some benzodiazepine derivatives, J. Phys. Theor. Chem. 14 (4) (2018) 343–352.

[50] D.A. Zainuri, M. Abdullah, S. Arshad, M.S.A. Aziz, G. Krishnan, H. Bakhtiar, I.A. Razaka, Crystal structure, spectroscopic and third-order nonlinear optical susceptibility of linear fused ring dichloro-substituent chalcone isomers, Opt. Mater. 86 (2018) 32–45, https://doi.org/10.1016/j.optmat.2018.09.032.

[51] J. Tauc, The Optical Properties of Solids, Academic Press, New York, 1966.

[52] S.R. Pilli, T. Banerjee, K. Mohanty, HOMO–LUMO energy interactions between endocrine disrupting chemicals and ionic liquids using the density functional theory: evaluation and comparison, J. Mol. Liq. 207 (2015) 112–124, https://doi.org/10.1016/j.molliq.2015.03.019.

[53] P.K. Chatteraj, S. Giri, S. Duley, Electrophilicity index, Chem. Rev. 111 (2011) 43–75, https://doi.org/10.1021/cr100149p.

[54] R.G. Pearson, Chemical hardness and density functional theory, J. Chem. Sci. 117 (2005) 369–377, https://doi.org/10.1007/BF02708340.

[55] Jose P. Abraham, D. Sajan, Venkataraya Shettigar, S.M. Dharmaprakash, I. Nemec, I. Hubert Joe, V.S. Jayakumar, Efficient π-electron conjugated push– pull nonlinear optical chromophore 1-(4-methoxyphenyl)-3-(3,4-dimethoxyphenyl)-2-propen-1-one: a vibrational spectral study, J. Mole. Struct. 917 (2009) 27–36, https://doi.org/10.1016/j.molstruc.2008.06.031.

[56] Y. Diwedi, G. Tamashiro, L.D. Boni, S.C. Zilio, Nonlinear optical characterization of dibenzoylmethane in solution, Opt Commun. 293 (2013) 119–124, https://doi.org/10.1016/j.optcom.2012.11.065.

[57] J.-J. Aaron, M. Maafi, C. Kersebet, C. Párkányi, M.S. Antonious, N. Motohashi, A solvatochromic study of new benzo[a]phenothiazines for the determination of dipole moments and specific solute-solvent interactions in the first excited singlet state, J. Photochem. Photobiol. Chem. 101 (1996) 127–136, https://doi.org/10.1016/s1010-6030(96)04442-5.

[58] A. Adenier, J.-J. Aaron, C. Párkányi, G. Deng, M. Sallah, Solvent effects on the electronic absorption and fluorescence emission spectra of merocyanine 540 – a biological probe, Heterocycl. Commun. 2 (1996), https://doi.org/10.1515/hc.1996.2.5.403.

[59] J.J. Aaron, C. Párkányi, A. Adenier, C. Potin, Z. Zajíčková, O.R. Martínez, J. Svoboda, P. Pihera, P. Váchal, Fluorescence properties and dipole moments of novel fused thienobenzofurans, Solvent and Structural Effects, Journal of Fluorescence 21 (2011) 2133–2141, https://doi.org/10.1007/s10895-011-0914-3.

[60] S.R. Maidur, P.S. Patil, S.V. Rao, M. Shkir, S.M. Dharmaprakash, "Experimental and computational studies on second-and third-order nonlinear optical properties of a novel D-π-A type chalcone derivative: 3-(4-methoxyphenyl)-1-(4-nitrophenyl) prop-2-en-1-one,", Opt Laser. Technol. 97 (2017) 219–228, https://doi.org/10.1016/j.optlastec.2017.07.003.

[61] E.D. Glendening, C.R. Landis, F. Weinhold, Natural bond orbital methods, Wiley Interdiscip. Rev. Comput. Mol. Sci. 2 (2011) 1–42, https://doi.org/10.1002/wcms.51.

[62] A.E. Reed, L.A. Cutis, F. Weinhold, Intermolecular interactions from a natural bond orbital, donor-acceptor viewpoint, Chem. Rev. 88 (1988) 899–926, https://doi.org/10.1021/cr00088a005.

[63] M.C. Sreenath, I.H. Joe, V.K. Rastogi, "Experimental and theoretical investigation of third-order nonlinear optical properties of azo dye 1-(2, 5-Dimethoxy-phenylazo)-naphthalen-2-ol by Z-scan technique and quantum chemical computations, Dyes Pigments 157 (2018) 163–178, https://doi.org/10.1016/j.dyepig.2018.04.044.

[64] N. Ozdemir, B. Eren, M. Dincer, Y. Bekdemir, Experimental and *ab initio* computational studies on 4-(1*H*-benzo[*d*]imidazole-2-yl)-*N,N*-dimethylaniline, Mol. Phys. 108 (2010) 13–24, https://doi.org/10.1080/00268970903476688.

[65] P. Politzer, J.S. Murray, The fundamental nature and role of the electrostatic potential in atoms and molecules, Theor. Chem. Acc. 108 (2002) 134–142, https://doi.org/10.1007/s00214-002-0363-9.

[66] F.J. Luque, J.M. Lopez, M. Orozco, Perspective on "Electrostatic interactions of a solute with a continuum. A direct utilization of ab initio molecular potentials for the prevision of solvent effects, Theor. Chem. Acc. 103 (2000) 343–345, https://doi.org/10.1007/s002149900013.

[67] N. Okulik, A.H. Joubert, Theoretical analysis of the reactive sites of non-steroidal anti-inflammatory drugs. Internet Elec-tron, J. Mol. Des. 4 (2005) 17–30.

[68] D. Lin-vien, N.B. Colthup, W.G. Fateley, J.G. Grasselli, The Hand Book of Infrared and Raman Characteristic Frequencies of Organic Molecules, Academic Press, New York, 1990.

[69] N.B. Colthup, L.H. Daly, S.E. Wiberley, Introduction to Infrared to and Raman Spectroscopy, Academic press, New York, 1990.

[70] B. Smith, Infrared Spectral Interpretation, a Systematic Approach, CRC, Washington, DC, 1999.

[71] L.J. Bellamy, The Infrared Spectra of Complex Molecules, third ed., Wiley, New York, 1975.

[72] G. Varsanyi, Assignments for Vibrational Spectra of Seven Hundred Benzene Derivatives vol. 1, Adam Hilger, London, 1974.

[73] G. Socrates, "Infrared and Raman characteristic group frequencies,", John Wiley & Sons Ltd, Chichester (2001).

[74] M. Snehalatha, C. Ravikumar, N. Sekar, V.S. Jayakumar, I.H. Joe, FT-Raman, IR and UV-visible spectral investigations and ab initio computations of a nonlinear food dye amaranth, J. Raman Spectrosc. 39 (2008) 928–936, https://doi.org/10.1002/jrs.1938.